PHYSICAL REVIEW A **96**, 063839 (2017)

Entanglement and asymmetric steering over two octaves of frequency difference

M. K. Olsen
School of Mathematics and Physics, University of Queensland, Brisbane, Queensland 4072, Australia and Quantum Science Otago and Dodd-Walls Centre for Photonic and Quantum Technologies, Department of Physics, University of Otago, Dunedin, New Zealand

(Received 9 July 2017; published 29 December 2017)

The development of quantum technologies which use quantum states of the light field interacting with other systems creates a demand for entangled states spanning wide frequency ranges. In this work we analyze a parametric scheme of cascaded harmonic generation which promises to deliver bipartite entangled states in which the two modes are separated by two octaves in frequency. This scheme is potentially very useful for applications in quantum communication and computation networks as well as providing for quantum interfaces between a wider range of light and atomic ensembles than is presently practicable. It doubles the frequency range over which entanglement is presently available.

DOI: 10.1103/PhysRevA.96.063839

I. INTRODUCTION

In this work we will show that cascaded second harmonic generation can produce bright entangled beams across a two-octave frequency range, which enlarges the available frequency difference for several important quantum technological applications. This will provide enhanced flexibility for quantum interfaces between light and atomic ensembles, as well as quantum state engineering, the entanglement of atomic ensembles, and quantum teleportation [1]. The availability of entanglement and Einstein-Podolsky-Rosen (EPR) steering over such a large frequency range will bring further flexibility to the linking of quantum processes at different wavelengths, for example, the telecommunications frequencies and atomic systems used in quantum information processing, particularly with quantum memory [2]. The system analyzed in this work doubles the frequency range of presently available technology, for which entanglement has been measured over a single octave [3].

The theory of the interaction of light fields at one frequency with nonlinear materials to produce fields at different frequencies goes back at least to Armstrong *et al.*, who produced a seminal work which included second and third harmonic generation [4]. That work did not consider fourth harmonic generation, possibly because the nonlinearity needed for a five-wave mixing process would be relatively weak. Despite this inherent weakness, and the difficulty of finding materials that are transparent over two octaves, Komatsu *et al.* successfully produced fourth harmonic from $Li_2B_4O_7$ crystal, with a conversion efficiency of 20% [5]. The advent of quasiperiodic superlattices meant that higher than second order processes were readily available, with Zhu *et al.* producing third harmonic by coupling second harmonic generation (SHG) and sum-frequency generation in 1997 [6]. Using $CsLiB_6O_{10}$, Kojima *et al.* were able to produce fourth harmonic at a 10 kHz repetition rate by 2000 [7]. Broderick *et al.* have produced fourth harmonic from a cascaded SHG process using a HeXLN crystal [8], which could be tuned for both processes at the same temperature. Chen *et al.* have produced ultraviolet outputs via cascaded SHG, beginning with an 800˜nm pump [9]. Südmeyer *et al.* produced fields at both second and fourth harmonics using an intracavity cascaded process with lithium triborate and barium borate crystals, with greater than 50% efficiency [10]. More recently, Ji *et al.* have generated light at 263 nm from a 1053 nm input, using KD^*P and $NH_4H_2PO_4$ crystals with noncritical phase matching [11]. The process which we analyze in this article now has a relatively long experimental history. Our theoretical contribution is to analyze the entangled outputs and show that cascaded harmonic generation can be used for useful quantum technologies spanning two octaves.

The theoretical examination of the quantum statistical properties of fourth harmonic generation began with Kheruntsyan *et al.*, who analyzed an intracavity cascaded frequency-doubler process [12]. The authors adiabatically eliminated the highest frequency mode to calculate squeezing in the remaining modes, while also finding self-pulsing in the intensities. Yu and Wang [13] performed an analysis of the system without any elimination, starting with the full positive-P representation [14] equations of motion. Linearizing around the steady-state solutions of the semiclassical equations, they performed a stability analysis and examined the entanglement properties using the method of symplectic eigenvalues [15].

In this work we extend previous analyses by integrating the full positive-P equations of motion in the intracavity configuration of cascaded harmonic generation. Using the standard input-output relations [16], we show that all three output fields can exhibit quadrature squeezing in both configurations and that the full quantum solutions for the field intensities can be qualitatively different from the classical predictions, meaning that care must be taken with any linearized analysis. We also use the Reid EPR criteria [17] to detect bipartite entanglement and EPR steering [18–20] in all three possible bipartitions. We find that as well as producing steering and entanglement across one octave for both transitions, the system can also be used to produce entangled states and asymmetric steering across two octaves of frequency difference.

II. HAMILTONIAN AND EQUATIONS OF MOTION

Our system, shown schematically in Fig. 1, consists of three fields interacting in nonlinear media, which could be either a periodically poled dielectric or two separate nonlinear crystals

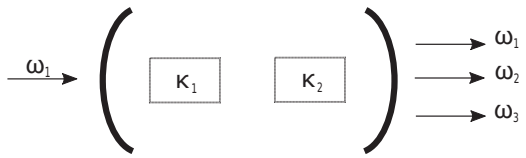

FIG. 1. Schematic of the system showing the nonlinear media inside an optical cavity and the input and output modes.

held in the same optical cavity. The equations of motion are the same for both. The fundamental field at ω_1, which will be externally pumped, is represented by $\hat{a}_1$. The second harmonic, at $\omega_2 = 2\omega_1$, is represented by $\hat{a}_2$, and the fourth harmonic, at $\omega_3 = 4\omega_1$, is represented by $\hat{a}_3$. The nonlinearity κ_1 couples the fields at ω_1 and ω_2, while κ_2 couples those at ω_2 and ω_3. The unitary interaction Hamiltonian in a rotating frame is then written as

$$\mathcal{H}_{\rm int} = \frac{i\hbar}{2}\left[\kappa_1\left(\hat{a}_1^2\hat{a}_2^\dagger - \hat{a}_1^{\dagger 2}\hat{a}_2\right) + \kappa_2\left(\hat{a}_2^2\hat{a}_3^\dagger - \hat{a}_2^{\dagger 2}\hat{a}_3\right)\right]. \quad (1)$$

For the intracavity configuration, we also have the pumping Hamiltonian,

$$\mathcal{H}_{\rm pump} = i\hbar(\epsilon\hat{a}_1^\dagger - \epsilon^*\hat{a}_1), \quad (2)$$

where ϵ represents an external pumping field, which is usually taken as coherent, although this is not necessary [21]. The damping of the cavity into a zero-temperature Markovian reservoir is described by the Lindblad superoperator

$$\mathcal{L}\rho = \sum_{i=1}^{3}\gamma_i(2\hat{a}_i\rho\hat{a}_i^\dagger - \hat{a}_i^\dagger\hat{a}_i\rho - \rho\hat{a}_i^\dagger\hat{a}_i), \quad (3)$$

where ρ is the system density matrix and γ_i is the cavity loss rate at ω_i. In this work we will treat all three optical fields as being at resonance with the optical cavity. In the intracavity configuration, only three modes need to be considered to give an accurate analysis of the system. Although the second and fourth harmonics can decay into pairs of nondegenerate modes that conserve energy, these will not be at resonance with the cavity and are therefore suppressed. The two nonlinear media are also phase matched for the harmonic generation process, and the three modes of interest are at resonance as well as being Bose enhanced. These are therefore the dominant frequencies, and theoretical analyses of intracavity second harmonic generation are known to not lose accuracy because of neglect of insignificant transitions. One example of this is found in Grosse *et al.* [3], where a two-mode analysis closely matched experimental results.

Following the usual procedures [22,23], we can derive equations of motion in the positive-P representation [14],

$$\begin{aligned}
\frac{d\alpha_1}{dt} &= \epsilon - \gamma_1\alpha_1 + \kappa_1\alpha_1^+\alpha_2 + \sqrt{\kappa_1\alpha_2}\,\eta_1,\\
\frac{d\alpha_1^+}{dt} &= \epsilon - \gamma_1^+\alpha_1^+ + \kappa_1\alpha_1\alpha_2^+ + \sqrt{\kappa_1\alpha_2^+}\,\eta_2,\\
\frac{d\alpha_2}{dt} &= -\gamma_2\alpha_2 + \kappa_2\alpha_2^+\alpha_3 - \frac{\kappa_1}{2}\alpha_1^2 + \sqrt{\kappa_2\alpha_3}\,\eta_3,\\
\frac{d\alpha_2^+}{dt} &= -\gamma_2\alpha_2^+ + \kappa_2\alpha_2\alpha_3^+ - \frac{\kappa_1}{2}\alpha_1^{+2} + \sqrt{\kappa_2\alpha_3^+}\,\eta_4,\\
\frac{d\alpha_3}{dt} &= -\gamma_3\alpha_3 - \frac{\kappa_2}{2}\alpha_2^2,\\
\frac{d\alpha_3^+}{dt} &= -\gamma_3\alpha_3^+ - \frac{\kappa_2}{2}\alpha_2^{+2},
\end{aligned} \quad (4)$$

noting that these have the same form in either Itô or Stratonovich calculus [24]. The complex variable pairs (α_i,α_j^+) correspond to the operator pairs $(\hat{a}_i,\hat{a}_j^\dagger)$ in the sense that stochastic averages of products converge to normally ordered operator expectation values, e.g., $\overline{\alpha_i^{+m}\alpha_j^n} \to \langle\hat{a}_i^{\dagger m}\hat{a}_j^n\rangle$. The η_j are Gaussian noise terms with the properties $\overline{\eta_i} = 0$ and $\overline{\eta_j(t)\eta_k(t')} = \delta_{jk}\delta(t-t')$. We note here that our equations are different from those used by Yu and Wang [13]. The sign change has no physical significance, but the different noise terms will have. Since the diffusion matrix of the Fokker-Planck equation is diagonal, we do not obtain complex noise terms. In fact, using their noise terms, the BB^T of their Eq. (11) would be different, and hence any predictions for output spectra would be different. We do not know of a method for obtaining a different diffusion matrix to the one we have used. Our stochastic equations were solved by numerical integration using a three-step predictor-corrector method, with the results being averaged over a large number of trajectories. The mean-field solutions required for the intracavity section below were found using MATLAB's ODE45.

III. QUANTUM CORRELATIONS IN THE TRAVELING-WAVE CONFIGURATION

Before we analyze the properties of the intracavity system, it is of interest to look at a simplified traveling wave configuration, using only the unitary Hamiltonian dynamics. The equations for this are found by removing the pumping and damping terms from Eq. (4). The time development of the intensities is shown in Fig. 2, both in the fully quantum picture and in a semiclassical approximation where the noise terms are removed from the equations. We see that the quantum dynamics are qualitatively different from the semiclassical solutions after some interaction time, an effect which has previously been found in SHG [25], third harmonic generation [26,27], and sum frequency generation [28]. This effect is purely due to the quantum nature of the fields. We note here that the ratio κ_2/κ_1 has a dramatic effect on the intensities, with N_1 almost vanishing before its revival when this ratio is set to unity, so that this could be interesting to investigate further.

For the same parameters as in Fig. 2 , we find that there is quadrature squeezing in all three fields during the initial interaction, as shown in Fig. 3. The disappearance of the squeezing after some time is reminiscent of many traveling-wave processes [25–28] and happens once down conversion becomes important. In order to detect entanglement, we can use either the Duan-Simon [29,30] or the Reid EPR criteria [17,18]. Since states exhibiting the EPR paradox are a strict subset of the entangled states [20], we will show results for the Reid EPR criteria, written in terms of products of inferred variances. We label these products EPR_{jk}, signifying that mode j can be steered by mode k. The two fields which violate the inequalities to the largest degree, i.e., $EPR_{jk} < 1$,

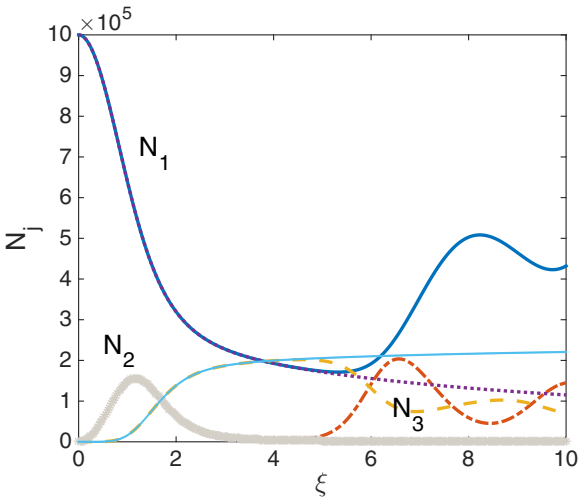

FIG. 2. Positive-P and classical solutions for intensities in the traveling-wave configuration, with $\kappa_1 = 0.005$, $\kappa_2 = 4\kappa_1$, and $N_1(0) = 10^6$. The quantum solutions are the lines which begin oscillations at $\xi \approx 5$. The dimensionless interaction time, ξ, is equal to $\kappa_1|\langle\alpha_1(0)\rangle|t$. The equations were averaged over 1.4×10^6 stochastic trajectories. All quantities in this and subsequent figures are dimensionless.

are the second and fourth harmonics, which exhibit asymmetric EPR steering [31–33], as shown in Fig. 4. We note here that steering and entanglement are found between other modes, and that the degree of violation of the inequalities depends on the actual parameters, but rather than investigate this further we will move to the intracavity case.

IV. STEADY-STATE CORRELATIONS FOR INTRACAVITY CONFIGURATION

In the intracavity configuration we find that the semiclassical and quantum solutions for the intensities are identical until a certain pump power, after which the system enters a self-pulsing regime [12,34]. We find that, much like the case

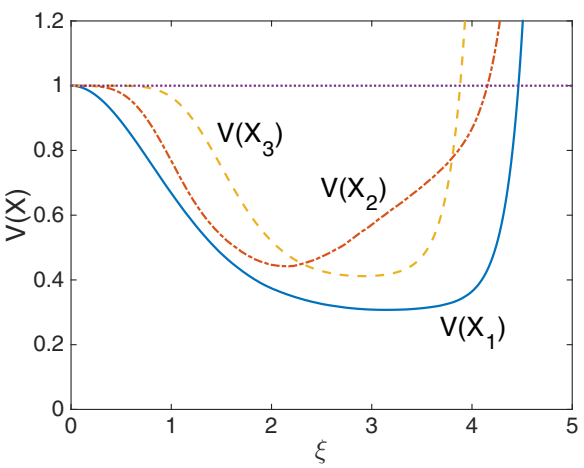

FIG. 3. Positive-P solutions for $\hat{X}$ quadrature variances in the traveling-wave configuration, with parameters as in Fig. 2. The line at 1 is a guide to the eye.

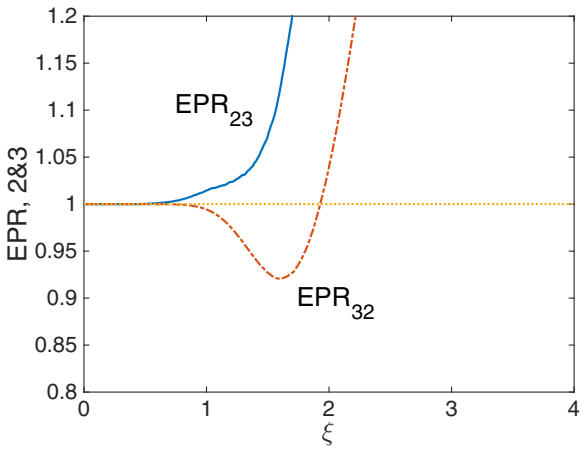

FIG. 4. Positive-P solutions for EPR steering between ω_2 and ω_3 in the traveling-wave configuration, with parameters as in Fig. 2. The line at 1 is a guide to the eye.

of intracavity third harmonic generation [27,35], the classical solutions overstate the amplitude of the pulsing. This is shown in Fig. 5 and does not happen in SHG, where the quantum and semiclassical solutions are identical. We note here that this low-amplitude pulsing is not an artifact of averaging over a low number of stochastic trajectories, with the results for the intensities not changing between averaging over 10^4 and 2×10^5 realizations. The difference from the behavior in standard SHG is presumably because there is a clear hard mode transition in that system, where two eigenvalues of the drift matrix become imaginary and conjugate. The eigenvalue spectra of this cascaded system is more complicated, with both imaginary and real parts for the eigenvalues. We were not able to find analytical solutions but have ensured numerically that the spectra given below are in a stable regime.

When nonlinear optical media are held inside a pumped optical cavity, the measured observables are usually the output spectral correlations, which are accessible using homodyne measurement techniques [16]. These are readily calculated

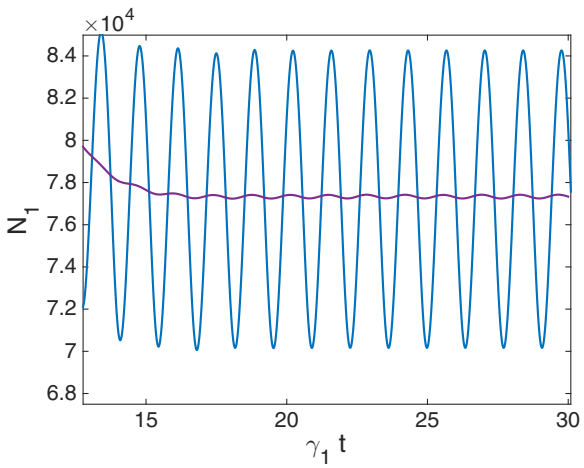

FIG. 5. Positive-P and classical solutions for N_1 in the self-pulsing regime, for $\kappa_1 = 0.005$, $\kappa_2 = 4\kappa_1$, $\gamma_1 = 1$, $\gamma_2 = \gamma_3 = \gamma_1/2$, and $\epsilon = 400$. The classical solution has the larger oscillations.

in the steady state by treating the system as an Ornstein-Uhlenbeck process [24]. In order to do this, we begin by expanding the positive-P variables into their steady-state expectation values plus delta-correlated Gaussian fluctuation terms:

$$\alpha_{ss} \rightarrow \langle \hat{a} \rangle_{ss} + \delta\alpha. \tag{5}$$

Given that we can calculate $\langle \hat{a} \rangle_{ss}$, we can then write the equations of motion for the fluctuation terms. The resulting equations are written for the vector of fluctuation terms as

$$d\delta\vec{\alpha} = -A\delta\vec{\alpha}dt + Bd\vec{W}, \tag{6}$$

where A is the drift matrix containing the steady-state solution, B is found from the factorisation of the diffusion matrix of the original Fokker-Planck equation, $D = BB^T$, with the steady-state values substituted, and $d\vec{W}$ is a vector of Wiener increments. As long as the matrix A has no eigenvalues with negative real parts, this method may be used to calculate the intracavity spectra via

$$S(\omega) = (A + i\omega)^{-1} D (A^{\mathrm{T}} - i\omega)^{-1}, \tag{7}$$

from which the output spectra are calculated using the standard input-output relations [16].

In this case

$$A = \begin{bmatrix} \gamma_1 & -\kappa_1\alpha_2 & -\kappa_1\alpha_1^* & 0 & 0 & 0 \\ -\kappa_1\alpha_2^* & \gamma_1 & 0 & -\kappa_1\alpha_1 & 0 & 0 \\ \kappa_1\alpha_1 & 0 & \gamma_2 & -\kappa_2\alpha_3 & -\kappa_2\alpha_2^* & 0 \\ 0 & \kappa_1\alpha_1^* & -\kappa_2\alpha_3^* & \gamma_2 & 0 & -\kappa_2\alpha_2 \\ 0 & 0 & \kappa_2\alpha_2 & 0 & \gamma_3 & 0 \\ 0 & 0 & 0 & \kappa_2\alpha_2^* & 0 & \gamma_3 \end{bmatrix}, \tag{8}$$

and D is a 6×6 matrix with $[\kappa_1\alpha_2, \kappa_1\alpha_2^*, \kappa_2\alpha_3, \kappa_2\alpha_3^*, 0, 0]$ on the diagonal. In the above, the α_j should be read as their steady-state values. Because we have parameterized our system using $\gamma_1 = 1$, the frequency ω is in units of γ_1. $S(\omega)$ is now in terms of quadratic products of the fluctuation operators. To express it in terms of the canonical quadratures, we calculate

$$S^q(\omega) = QSQ^T, \tag{9}$$

where Q is the block diagonal 6×6 matrix constructed from

$$q = \begin{bmatrix} 1 & 1 \\ -i & i \end{bmatrix}. \tag{10}$$

$S^q(\omega)$ then gives us the products we require to construct the output spectral variances and covariances for modes i and j as, for example,

$$V(X_i, X_j) = \delta_{ij} + \sqrt{\gamma_i\gamma_j}\left(S^q_{2i-1,2j-1} + S^q_{2j-1,2i-1}\right). \tag{11}$$

For our analysis we have chosen parameters which were found via numerical experimentation to optimize the results in terms of entanglement of the output fields. This required $\kappa_2 > \kappa_1$ and $\gamma_1 > \gamma_{2,3}$ and would therefore require a careful matching of the nonlinear material to the cavity mirrors. Given the wide range of materials covered in our introduction, we believe this to be possible. We also note that this is the opposite of the regime analyzed by Kheruntsyan *et al.* [12], where the high-frequency mode could be adiabatically eliminated since γ_3 was much larger than the other loss rates. We note here that, since we have set $\gamma_1 = 1$, all the other parameters are scaled in terms of this quantity.

The first property we examine here is again the quadrature variances. As shown in Fig. 6, a degree of squeezing comparable to that found in SHG [36] is available in all three modes. We also find that EPR steering exists for all three possible bipartitions. That which violates the inequality by the greatest amount is the grouping of mode 2 with mode 3, as shown in Fig. 7. This violation necessarily also means that

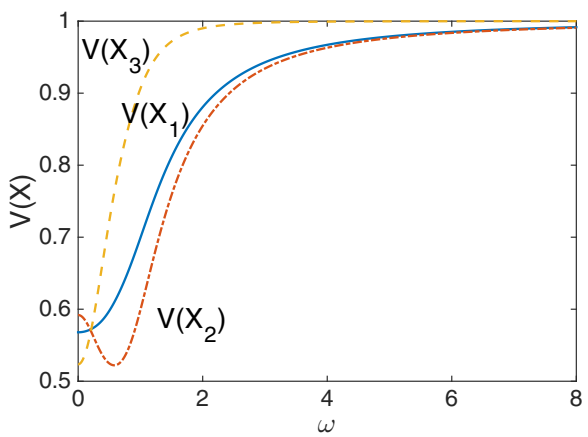

FIG. 6. $\hat{X}$ quadrature variances, for $\kappa_1 = 0.005$, $\kappa_2 = 4\kappa_1$, $\gamma_1 = 1$, $\gamma_2 = \gamma_3 = \gamma_1/2$, and $\epsilon = 105$. The frequency axis is in units of the line width of the fundamental, γ_1.

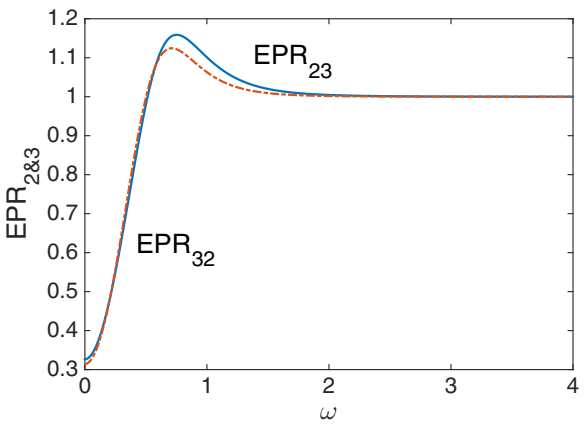

FIG. 7. The Reid criteria for steering between ω_2 and ω_3, for the same parameters as Fig. 6.

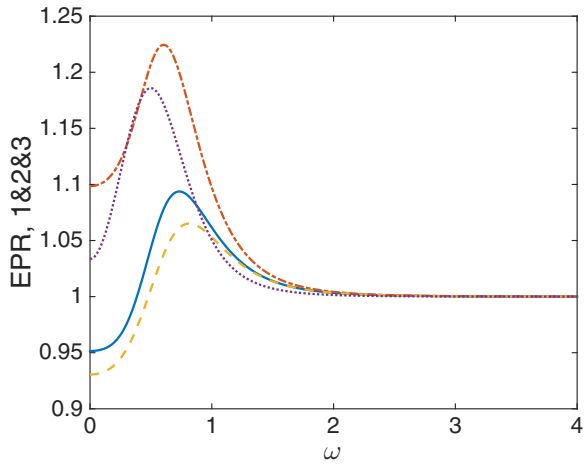

FIG. 8. The Reid criteria for steering between modes 1 and 2, and 1 and 3, for the same parameters as Fig. 6. The solid line is EPR_{12}, the dash-dotted line is EPR_{21}, the dashed line is EPR_{13}, and the dotted line is EPR_{31}.

these two modes are entangled, across one octave of frequency difference. Nonclassical correlations have previously been predicted over such a frequency ratio [37], while entanglement and EPR steering have been predicted in SHG in both traveling wave [38] and intracavity configurations [32], and experimentally achieved via an intracavity $\chi^{(2)}$ medium pumped at both the fundamental and harmonic frequencies [3]. Depending on the pump frequency, the steering found here could extend from the optical to the ultraviolet and be useful for multiplexing in quantum communication applications [39].

When we consider the fundamental and its entanglement with the second and fourth harmonics, we again find that entanglement is present for both bipartitions, as shown by the EPR steering results in Fig. 8. In this case we find that the steering in both bipartitions is asymmetric, with the fundamental being able to steer the higher modes but these being unable to steer the fundamental. Since this system is Gaussian, the Reid criteria are both necessary and sufficient to demonstrate this feature.

V. CONCLUSION

In conclusion, we have proposed and analyzed a cascaded $\chi^{(2)}$ system which has outputs that show bipartite entanglement and EPR correlations over a two octave frequency range. With an input at the 1550˜nm frequency, for example, this could produce entangled modes in both the infrared and visible ranges. With a 1064˜nm input, the output frequencies range from infrared through the visible, to ultraviolet. This frequency range lends itself to multiplexing applications and the interfacing of light and atoms. The existence of asymmetric EPR steering between the fundamental and the higher modes makes this device even more versatile, with other possible uses in quantum key distribution and continuous variable teleportation. Numerical experimentation found that the best degree of quantum correlation occurs when the system is carefully engineered so that the nonlinearity for second to fourth harmonic generation is greater than that which links the fundamental and the first harmonic. Cavity losses which are lower at the higher frequencies are also preferable.

[1] K. Hammerer, A. S. Sørensen, and E. S. Polzik, Rev. Mod. Phys. **82**, 1041 (2010).
[2] B. Julsgaard, J. Sherson, I. Cirac, L. Fiurášek, and E. S. Polzik, Nature (London) **432**, 482 (2004).
[3] N. B. Grosse, S. Assad, M. Mehmet, R. Schnabel, T. Symul, and P. K. Lam, Phys. Rev. Lett. **100**, 243601 (2008).
[4] J. A. Armstrong, N. Bloembergen, J. Ducuing, and P. S. Pershan, Phys. Rev. **127**, 1918 (1962).
[5] R. Komatsu, T. Sugarawa, K. Sassa, N. Sarukura, Z. Liu, S. Izumida, Y. Segawa, S. Uda, T. Fukuda, and K. Yamanouchi, Appl. Phys. Lett. **70**, 3492 (1997).
[6] S. Zhu, Y. Zhu, and N. Ming, Science **278**, 843 (1997).
[7] T. Kojima, S. Konno, S. Fujikawa, K. Kasui, K. Yoshizawa, Y. Mori, T. Sasaki, M. Tanaka, and Y. Okada, Opt. Lett. **25**, 58 (2000).
[8] N. G. R. Broderick, R. T. Bratfalean, T. M. Monro, and D. J. Richardson, J. Opt. Soc. Am. B **19**, 2263 (2002).
[9] C. Chen, J. Lu, T. Togashi, T. Suganuma, T. Sekikawa, S. Watanabe, Z. Xu, and J. Wang, Opt. Lett. **27**, 637 (2002).
[10] T. Südmeyer, Y. Imai, H. Masuda, N. Eguchi, M. Saito, and S. Kubota, Opt. Express **16**, 1546 (2008).
[11] S. Ji, F. Wang, L. Zhu, X. Xu, Z. Wang, and X. Sun, Sci. Rep. **3**, 1605 (2013).
[12] K. V. Kheruntsyan, G. Yu. Kryuchkyan, N. T. Mouradyan, and K. G. Petrosyan, Phys. Rev. A **57**, 535 (1998).
[13] Y. Yu and H. Wang, J. Opt. Soc. Am. B **28**, 1899 (2011).
[14] P. D. Drummond and C. W. Gardiner, J. Phys. A **13**, 2353 (1980).
[15] A. Serafini, G. Adesso, and F. Illuminati, Phys. Rev. A **71**, 032349 (2005).
[16] C. W. Gardiner and M. J. Collett, Phys. Rev. A **31**, 3761 (1985).
[17] M. D. Reid, Phys. Rev. A **40**, 913 (1989).
[18] A. Einstein, B. Podolsky, and N. Rosen, Phys. Rev. **47**, 777 (1937).
[19] E. Schrödinger, Proc. Cam. Philos. Soc. **31**, 555 (1935).
[20] H. M. Wiseman, S. J. Jones, and A. C. Doherty, Phys. Rev. Lett. **98**, 140402 (2007).
[21] E. Marcellina, J. F. Corney, and M. K. Olsen, Opt. Commun. **309**, 9 (2013).
[22] D. F. Walls and G. J. Milburn, *Quantum Optics* (Springer-Verlag, Berlin, 1995).
[23] C. W. Gardiner and P. Zoller, *Quantum Noise* (Springer-Verlag, Heidelberg, 2000).
[24] C. W. Gardiner, *Handbook of Stochastic Methods* (Springer, Berlin, 1985).
[25] M. K. Olsen, R. J. Horowicz, L. I. Plimak, N. Treps, and C. Fabre, Phys. Rev. A **61**, 021803 (2000).
[26] M. K. Olsen, L. I. Plimak, and M. Fleischhauer, Phys. Rev. A **65**, 053806 (2002).
[27] M. K. Olsen, arXiv:1706.05174.
[28] M. K. Olsen and A. S. Bradley, Phys. Rev. A **77**, 023813 (2008).

[29] L.-M. Duan, G. Giedke, J. I. Cirac, and P. Zoller, Phys. Rev. Lett. **84**, 2722 (2000).
[30] R. Simon, Phys. Rev. Lett. **84**, 2726 (2000).
[31] S. L. W. Midgley, A. J. Ferris, and M. K. Olsen, Phys. Rev. A **81**, 022101 (2010).
[32] M. K. Olsen, Phys. Rev. A **88**, 051802 (2013).
[33] V. Händchen, T. Eberle, S. Steinlechner, A. Samblowski, T. Franz, R. F. Werner, and R. Schnabel, Nat. Photon. **6**, 598 (2012).
[34] K. J. McNeil, P. D. Drummond, and D. F. Walls, Opt. Commun. **27**, 292 (1978).
[35] S. T. Gevorkyan, G. Yu. Kruchkyan, and K. V. Kheruntsyan, Opt. Commun. **134**, 440 (1997).
[36] M. J. Collett and D. F. Walls, Phys. Rev. A **32**, 2887 (1985).
[37] M. K. Olsen and R. J. Horowicz, Opt. Commun. **168**, 135 (1999).
[38] M. K. Olsen, Phys. Rev. A **70**, 035801 (2004).
[39] C. Baune, J. Gniesmer, S. Kocsis, C. E. Vollmer, P. Zell, J. Fiurášek, and R. Schnabel, Phys. Rev. A **93**, 010302 (2016).